JACS
JOURNAL OF THE AMERICAN CHEMICAL SOCIETY
Communication
pubs.acs.org/JACS

Molecular Structure, Spectroscopy, and Photoinduced Kinetics in Trinuclear Cyanide Bridged Complex in Solution: A First-Principles Perspective

Zilong Zheng,[†] Arun K. Manna,[†] Heidi P. Hendrickson,[‡] Morgan Hammer,[‡] Chenchen Song,[‡] Eitan Geva,*[,‡] and Barry D. Dunietz*[,†]

[†]Department of Chemistry, Kent State University, Kent, Ohio 44242, United States
[‡]Department of Chemistry, University of Michigan, Ann Arbor, Michigan 48120, United States

Supporting Information

ABSTRACT: We investigate the molecular structure of the solvated complex, $[(NC)_6Fe-Pt(NH_3)_4-Fe(CN)_6]^{4-}$, and related dinuclear and mononuclear model complexes using first-principles calculations. Mixed nuclear complexes in both solution and crystal phases were widely studied as models for charge transfer (CT) reactions using advanced spectroscopical and electrochemical tools. In contrast to earlier interpretations, we find that the most stable gas phase and solvated geometries are substantially different from the crystal phase geometry, mainly due to variance in the underlying oxidation numbers of the metal centers. Specifically, in the crystal phase a Pt(IV) metal center resulting from Fe ← Pt backward electron transfers is stabilized by an octahedral ligand field, whereas in the solution phase a Pt(II) metal complex that prefers a square planar ligand field forms a CT salt by bridging to the iron complexes through long-range electrostatic interactions. The different geometry is shown to be consistent with spectroscopical data and measured CT rates of the solvated complex. Interestingly, we find that the experimentally indicated photoinduced process in the solvated complex is of backward CT (Fe ← Pt).

Photoinduced charge transfer (CT) processes within molecular systems are prevalent[1−3] as they play key roles in a variety of biological systems[4−8] and in developing technologies.[9−11] Transition metal mixed nuclear complexes have been central in experimental studies used to develop our understanding of electron transfer processes.[12] Cyanide-bridged multinuclear complexes in particular are widely pursued as a means to synthesize materials for diverse applications, where photoinduced, internuclear CTs are indicated in spectroscopical and electrochemical measurements.[12−18]

In this report, we consider a trinuclear complex synthesized by combining $Pt^{(II)}(NH_3)_4(NO_3)_2$ and $K_3Fe^{(III)}(CN)_6$,[13,19] the latter of which has been found to dissociate upon photoexcitation to yield ferricyanide.[13,14,20,21] Interpretations of available experimental studies suggest the formation of a trinuclear complex described as $[(NC)_6Fe^{(II)}-Pt^{(IV)}(NH_3)_4-Fe^{(II)}(CN)_6]^{4-}$ (abbreviated below as $Fe^{(II)}Pt^{(IV)}Fe^{(II)}$). Upon photoexcitation $[(NC)_6Fe^{(III)}-Pt^{(II)}(NH_3)_4-Fe^{(III)}(CN)_6]^{4-}$ (abbreviated below as $Fe^{(III)}Pt^{(II)}Fe^{(III)}$) is believed to result from two forward electron transfers (Fe → Pt).[14,21]

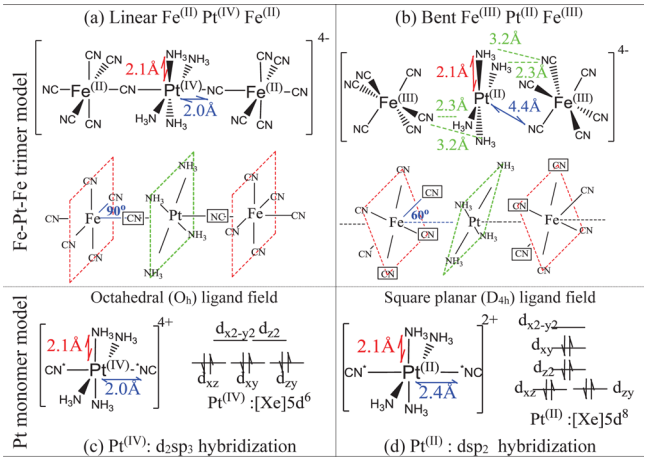

Figure 1. Molecular structures of optimized trimetal complexes, linear (a) and bent (b) structures (atomic coordinates are provided in SI Table S1a). Middle panel: Bridging ligands are indicated by squares. Lower panel: Ligand field and optimized (c) $Pt^{(IV)}$ and (d) $Pt^{(II)}$ monomer models. (*NC is an isocyanide radical in the mononuclear Pt complex. Corresponding dimers are analyzed in SI Table S2 and Figure S1.)

Our primary goal in this work is to determine the ground state electronic structure and geometry of the trimer complex and validate our assignment against available spectroscopical measurements. In addition, we investigate the photoinduced CT kinetics and compare with measured rates.

To understand the relationships between the trinuclear complex structure, ligand fields of the metallic centers, and the electronic density, we consider the following two key configurations (illustrated in Figure 1):

1) The single ligand-bridged structure (hereafter referred to as the linear geometry), where a single cyano ligand connects two metal centers in a straight line to form a trinuclear complex with a D_{4h} point group symmetry, is found to correspond to $Fe^{(II)}Pt^{(IV)}Fe^{(II)}$.
2) The multiple ligand-bridged structure (hereafter referred to as the bent geometry), where three cyano ligands take

Received: April 26, 2014
Published: November 2, 2014

   dx.doi.org/10.1021/ja507131q | J. Am. Chem. Soc. 2014, 136, 16954−16957

part in bridging each pair of the metal centers to form a bent orientation of each Fe−CN bond to the Fe−Pt axis with a lower point symmetry of C_2, is found to correspond to $Fe^{(III)}Pt^{(II)}Fe^{(III)}$.

Our main finding is that the bent geometry is more stable. We first rationalize this novel assignment by considering the underlying ligand fields and oxidation numbers. The novel structural assignment of the trinuclear complex is confirmed by validation against available experimental data. While the linear structure reproduces well the solid-phase X-ray resolved data, the bent structure is associated with calculated vibrational and electronic spectra that are more consistent with the available experimental measurements of the solvated complex. We emphasize that the assignment of the trinuclear complex in solution to the bent structure contradicts earlier interpretations of related experimental studies[18] and in particular those concerning the nature of the photoinduced CT.[16]

The optimized geometries are obtained via DFT with the B3LYP functional.[22,23] Solvation was modeled via the polarizable continuum model (PCM)[24] with switching Gaussians.[25,26] We find the electronic density of the bent structure to involve two uncoupled open shell iron centers (Fe^{III}). We treat the bent structure as a triplet, where the open-shell singlet is confirmed to be degenerate in energy (higher spin states are found to be higher in energy). For the open shell calculations we used unrestricted spin version of DFT. We use 6-31G(d) basis set for H, N, C and Fe atoms, and the all-electron SARC-ZORA basis set for the Pt atom unless otherwise noted. Table 1 compares the energies of the two structures at the gas and water solution. A more complete basis set study confirming the greater relative stability of the bent structure is included in Supporting Information (SI) Table S3, which analyzes the effect of polarization and diffuse functions using the 6-31+G(d,p) basis set. Relativistic effects due to the large Pt atom are gauged using the Stuttgart ECP,[27] where only small shortening of Pt−N ligand bonds[28] are found. All the Pt−N ligand bonds are shortened by less than 0.06 Å (see SI Table S3).

Key structural parameters of the two geometries are listed in Table 2 along with those of the measured X-ray crystal structure (atomic coordinates are listed in SI Table S1a). Electronic excited state energies were obtained using TDDFT/BNL within PCM with range switching parameters evaluated using the J_2 scheme[29] with PCM included (linear and bent parameters are γ = 0.038 and 0.004 $bohr^{-1}$, respectively). We also report calculated vibrational spectra and photoinduced CT rates via the semi-classical Marcus expression.[30] All calculations, unless otherwise stated, were implemented using Q-Chem 4.0.[31]

The linear geometry is consistent with the measured X-ray crystal structure, which revealed a single CN bridged complex.[13] The calculated Pt−NC (isocyanide ligand) bond lengths (2.04 Å) and orientations are in excellent agreement with the experimental values, with only up to 0.06 Å overestimation of bond length for the bridging ligands.

The bent geometry, which is inconsistent with the crystal structure, nevertheless provides for dramatically improved agreement with measured spectra of the solvated phase complex compared to the linear geometry. In the bent structure the Fe and Pt centers are bridged by three CN ligands, resulting in a substantial elongation of the Pt−NC bonds to 4.41 Å. The bridging CN ligands form a 62° angle to the Fe−Pt axis in contrast to the parallel arrangement of the bridging ligands in the linear geometry. Namely, we find that the bending refers to the angle of the bridging ligands to the Fe−Pt axis, while the Fe−Pt−Fe axis is linear in both structures.

Table 1. Adiabatic Ground State Energy Differences[a]

	gas phase	water solution
$E_{linear}-E_{bent}$	44.5	25.3

[a]6-31+G(d,p) level (Kcal/mol).

Table 2. Charges and Key Structural Features in Solution[a]

	Linear: $Fe^{+2}Pt^{+4}Fe^{+2}$	Bent: $Fe^{+3}Pt^{+2}Fe^{+3}$
Charge of ligated metal center	$(NC)_5Fe-CN^b$: −3.65(−3.5[c])	$(NC)_6Fe$: −3.0(−3.0[c])
	$NC^b-Pt(NH_3)_4-NC^b$: 3.3(3.0[c])	$Pt(NH_3)_4$: 2.0(2.0[c])
Length: Pt−NH_3	2.12 (2.08[d]) Å	2.14 Å
Length: Pt−NC	2.04 (1.97[d]) Å	4.41 Å
Angle: NC−Fe−Pt	90° (89°[d])	62°

[a]Optimized at the B3LYP/6-31+G(d,p) level with PCM. (The 6-31G(d) structure is consistent). [b]Bridged cyanide charges are shared by Fe and Pt centers. [c]Formal charge. [d]Crystal X-ray structure.[13]

We emphasize that the two structures are chosen following their physical significance, where the linear geometry represents the crystal structure and the bent geometry reflects the ligand orientation following electron transfers from the Fe centers to the Pt center. Accordingly, the change in Pt oxidation number, that determines the preferred ligand field, accounts for the substantial differences between the two structures. We begin by inspecting the specific coordination schemes involved in the corresponding two structures:

1) In the linear structure, composed of $Fe^{(II)}(CN)_6$ and $Pt^{(IV)}(NH_3)_4(NC)_2$ complexes, both metal centers involve d^6 electronic configuration that prefers octahedral ligand field with low spin closed-shell level splitting. The bridging CN molecules act as cyanide and isocyanide ligands to the Fe and Pt centers, respectively (see Figure 1a).
2) In the bent structure, composed of $Fe^{(III)}(CN)_6$ and $Pt^{(II)}(NH_3)_4$ complexes, the $Fe^{(III)}$ and $Pt^{(II)}$ centers involve d^5 and d^8 electronic configurations that prefer octahedral and square planar ligand fields, respectively. The bridging ligands contribute only to the Fe center ligand fields (see Figure 1b).

We point out that our ground state analysis of the two structures associating a $Pt^{(IV)}$ and a $Pt^{(II)}$ center to the linear and bent geometries, respectively, is confirmed using both Mulliken charges and Lowdin population analysis of the converged electronic densities in solvated phases (see complete details in SI Table S4 and summary in Table 2).

Thus, our ligand-field analysis, which associates the bent geometry with a square planar ligated $Pt^{(II)}$ center, explains that the elongation of the Pt−isocyanide bonds is related to long-range electrostatic interactions between the Pt center and three isocyanide molecules on each side. The linear structure, consisting of an octahedral ligated $Pt^{(IV)}$ center, is consistent with a single bridging ligand for each side in accordance with the X-ray crystal structure.

Importantly, the bent geometry is found to be 25 kcal/mol more stable than the linear geometry, which indicates that at room temperature all molecular complexes are bent. The stability of the bent structure, with the elongated bridging bonds, relative to the linear structure is in spite a weakened binding energy, which nevertheless explains well the experimental observation of the complex to photodissociate and yield ferricyanide.[13] The

dx.doi.org/10.1021/ja507131q | J. Am. Chem. Soc. 2014, 136, 16954−16957

greater stability of the bent geometry results from the dissociation limits of both structures as set by their corresponding oxidation numbers (see detailed energetics in SI Table S5).

To further validate that the bent structure (i.e., a square planar ligand field) is more stable with a $Pt^{(II)}$ center than $Pt^{(IV)}$, we turn to consider several simplified models. We analyze single Pt complexes with four NH_3 and two isocyanide ligands that correspond to the Pt center in the trimer complex. We confirm that the $Pt^{(II)}$ complex derived from the bent structure results in a square planar ligand field with the four NH_3 molecules acting as strong ligands, and the isocyanides interact only through weaker long-range forces at 2.4 Å (see Figure 1d). We find that the $Pt^{(IV)}$ complex derived from the linear structure results in an octahedral ligand field, where the isocyanides participate as strong ligands with 2.1 Å bond distances (see Figure 1c).

We also confirm the relationship between structure and oxidation numbers in related dinuclear models, where one of the Fe complexes is replaced by a NH_3 ligand (see SI Table S6). The Pt–NC bond is also elongated in the bent dimer model, representing a forward charge polarization.

The bent structure is also stabilized through energetic effects that are beyond the simplistic ligand field analysis. The extended bonding of the bridging CN ligands in the bent geometry essentially reflects a CT salt that is stabilized predominantly by long-range, ionic, electrostatic interactions. The Fe–Pt distance in the bent geometry was found to be 5.5 Å, which is slightly longer than the bonding in the linear geometry of 5.1 Å. Further stabilization in the bent structure is due to hydrogen bonding of all four amines with bridging cyano ligands with bond lengths of 2.3 and 3.2 Å (see Figure 1b). The total hydrogen bond energies were found to be 3.5 kcal/mol, via consideration of the CN···NH_3 dimers derived from the bent geometry. The bonding in a fully optimized CN···NH_3 dimer was found to be 1.8 kcal/mol. The CN ligands that participate in the hydrogen bonding are also involved in bridging to the Pt center (see middle panel of Figure 1). Similar stabilization due to hydrogen bonding has been indicated in other solvated trinuclear complexes that involve single CN bridging ligands.[12] In contrast, we find that the Fe–Pt–Fe structural constraints in the linear geometry forbid the formation of such hydrogen bonds.

Next, we validate the bent structure assignment against available experimental data. Both the trimer and the dimer bent structures are more consistent with the measured absorption and vibrational spectra.[21,32] While we focus in this communication on the trimer complex, for completeness the dimer spectra is provided in the SI. (The absorption energies and vibrational frequencies are listed in SI Table S7.)

Indeed, the vibrational spectra confirm the formation of a trimer complex, where the CN stretches are found to be red-shifted in comparison to the spectra of the single iron complex.[16,17] As shown in Figure 2, the experimental vibrational spectra[16−18] have four main bands of CN vibrations in the 2050–2116 cm^{-1} range. The calculated spectra for the bent structure, with a range of 2042–2112 cm^{-1}, are therefore more consistent with the experimental data than the calculated spectra for the linear structure with the 1936–2039 cm^{-1} range. In addition, the measured energy splitting between the different bands is more accurately achieved for the bent structure. Further support for the bent trimer geometry assignment is provided by recent evidence of a 60° tilted orientation of CN vibrations to the complex dipole.[18] The bent geometry offers a molecular level understanding of the indicated tilted CN stretches.

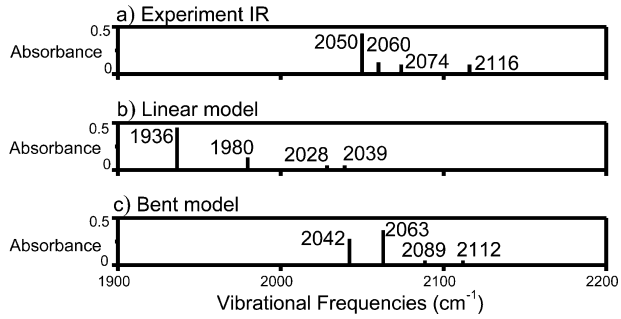

Figure 2. Experimental[16] (a) and calculated (b,c) vibrational spectrum (CN stretches). Frequencies are listed in SI Table S8.

Table 3. Absorption Energies (eV)

linear structure	bent structure	measured[13]
2.85 (0.1279)	3.01 (3.5446)	2.92 (2365 M^{-1} cm^{-1})
4.41 (0.2974)	3.83 (0.3303)	3.90 (2090 M^{-1} cm^{-1})

In parenthesis: Calculated oscillator strengths and measured molar absorptivities.

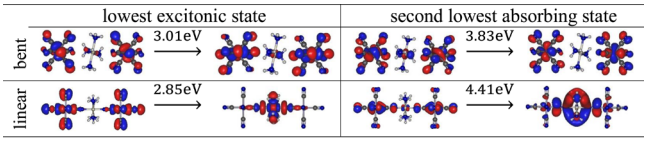

Figure 3. Natural transition orbitals (NTOs) describing the absorbing excited states calculated by TDDFT/BNL.

We now turn to the question of which structure is consistent with the electronic absorption spectrum. Formation of the trimer complex is also indicated by its signature on the absorption spectra, which differs from the spectra of the single metal complexes.[13,14,16,17] The calculated excitation energies and corresponding oscillator strengths for the linear and bent trimer structures are compared with the solution-phase experimental values[13] in Table 3. The orbitals describing the two lowest absorbing states in both structures are provided in Figure 3. (For completeness we include B3LYP dimer and trimer excitation energies in SI Table S9.) For the bent and linear trimer, we find that the lowest absorption state is similar between both geometries and in relatively good agreement with the experimental value (within 0.1 eV). However, the second excited state energy is matched quite well only by the bent structure, as it is significantly overestimated by the linear structure. In addition, the bent structure spectra are more consistent with the measured oscillator strength trend for the two low lying absorbing states, while the linear structure reflects an opposing trend (Table 3). We therefore find that the bent geometry is associated with calculated spectra that is much more consistent with available solution-phase spectroscopic data, in comparison to the calculated spectra of the linear structure.

We next consider the rate constant of photoinduced charge transfer that was measured at 9.09×10^{12} s^{-1}.[16] For modeling the photoinduced kinetics, we find a nonvanishing coupling between an absorbing excited state and a CT state *only* for the bent structure; no such coupling terms are found for the linear structure. These trends were determined by both the fragment charge difference[33] and the generalized Mulliken–Hush[34] scheme for calculating electronic coupling (with $V_{coupling}$ = 0.023 and 0.028 eV, respectively). The coupled CT state within

dx.doi.org/10.1021/ja507131q | J. Am. Chem. Soc. 2014, 136, 16954–16957

the bent structure involves backward CT from the Pt center to the Fe centers. The corresponding reorganization energies (E_r) and the reaction free energy (ΔE) confirm that the semiclassical picture, Marcus theory of photoinduced CT, is adequate since $E_r > |\Delta E|$. In calculating the E_r and the ΔE, we implement charge constrained DFT[35,36] with PCM parametrized by the TDDFT description of the CT state (see further detail in SI Figure S2). We find that backward CT for the bent geometry is associated with a rate constant of 6.62×10^{12} s^{-1}, which is in good agreement with experiment. The rate constant was determined via the semiclassical expression

$$k_{\mathrm{Marcus}} = \frac{|V_{\mathrm{coupling}}|^2}{\hbar}\sqrt{\frac{\pi}{k_B T E_r}}\, e^{-E_a/k_B T} = 6.62 \times 10^{12}\ s^{-1}$$

where $E_a = (\Delta E + E_r)^2/4E_r$ is the activation energy ($\Delta E = -1.05$ eV and $E_r = 1.21$ eV).

To conclude, we investigate a complex containing Fe−Pt−Fe metal centers bridged by CN ligands. Such multiple-metal complexes have been widely studied as models for photoinduced electron transfer reactions. Our calculations indicate that the structure of the trimer complex in the spectrally relevant solution phase (as well as the gas phase) should be assigned to the bent configuration, which differs substantially from the corresponding crystal phase structure. In particular, we find that the electronic distribution of the bent structure is well described as involving $Pt^{(II)}$ and two $Fe^{(III)}$ centers. Our novel assignment is confirmed by contrasting against available experimental data.

We find that the solvated ground state of the trimer Fe−Pt−Fe complex involves elongated Pt−isocyanide (Pt−NC) bonds, reflecting a square planar ligand field around a d^8 $Pt^{(II)}$ center. The solvated structure is therefore found to be substantially different from the linear structure that corresponds well to the crystal structure of the complex. We also note the good agreement between calculated electronic and vibrational spectra of the bent structure and experimental measurements. Finally, we find that, for the bent structure, the lowest $\pi\pi^*$ excited state is strongly coupled to a backward CT state (at 3.17 eV, Pt → Fe), resulting in a CT rate that is in good agreement with the measured value. In the linear structure we find no alternative CT states to be coupled to absorbing states.

■ ASSOCIATED CONTENT

Supporting Information

Cartesian coordinates of the models, ligand field orbital diagrams, and additional spectral data for the different complexes. This material is available free of charge via the Internet at http://pubs.acs.org.

■ AUTHOR INFORMATION

Corresponding Authors

*eitan@umich.edu.

*bdunietz@kent.edu.

Notes

The authors declare no competing financial interest.

■ ACKNOWLEDGMENTS

B.D.D. and Z.Z. thank Prof. Khalil for numerous discussions and for introducing the interesting system. B.D.D. and Z.Z. are grateful to Songping Huang for critical comments and useful discussions. Work by B.D.D. and A.M. was supported by a DOE-BES award through the Chemical Sciences Geosciences and Biosciences Division (DE-SC0004924), DE-FG02-10ER16174. Z.Z. was supported by the Center for Solar and Thermal Energy Conversion, an Energy Frontier Research Center funded by the US DOE under Award No. DE-SC0000957. H.H. acknowledges a graduate research fellowship by the NSF under Grant No. DGE 0718128. M.H. and C.S. were supported by the University of Michigan Chemistry Research Experience for Undergraduates program. We are also grateful to generous resource allocations on the Ohio Supercomputer Center and the Kent State University, College of Arts and Sciences Computing Cluster.

■ REFERENCES

(1) Thompson, A.; Ahn, T.-S.; Justin, K. R.; Thayumanavan, T. S.; Martínez, T. J.; Bardeen, C. J. *J. Am. Chem. Soc.* **2005**, *127*, 16348.
(2) Reinheimera, E. W.; Galan-Mascarosb, J.; Dunbar, K. R. *Synth. Met.* **2009**, *159*, 45.
(3) Jailaubekov, A. E.; Willard, A. P.; Tritsch, J. R.; Chan, W.-L.; Sai, N.; Gearba, R.; Kaake, L. G.; Williams, K. J.; Leung, K.; Rossky, P. J.; Zhu, X.-Y. *Nat. Mater.* **2013**, *12*, 66.
(4) Jortner, J.; Bixon, M.; Langenbacher, T.; Michel-Beyerle, M. E. *Proc. Natl. Acad. Sci. U.S.A.* **1998**, *95*, 12759−12765.
(5) O'Neill, M. A.; Barton, J. K. *Proc. Natl. Acad. Sci. U.S.A.* **2002**, *99*, 16543.
(6) Lewis, D. F.; Liu, J.; Weigel, W.; Rettig, W.; Kurnikov, I. V.; Beratan, N. *Proc. Natl. Acad. Sci. U.S.A.* **2002**, *99*, 12536.
(7) Bergeron, F.; Houde, D.; Hunting, D. J.; Wagner, J. R. *Nucleic Acids Res.* **2004**, *32*, 6154.
(8) Takaya, T.; Su, C.; Harpe, K. d. L.; Crespo-Hernandez, C. E.; Kohler, B. *Proc. Natl. Acad. Sci. U.S.A.* **2008**, *105*, 10285.
(9) Bredas, J.-L.; Norton, J. E.; Cornil, J.; Coropceanu, V. *Acc. Chem. Res.* **2009**, *42*, 1691.
(10) Deibel, C.; Strobel, T.; Dyakonov, V. *Adv. Mater.* **2010**, *22*, 4097.
(11) Gong, X.; Tong, M.; Brunetti, F. G.; Seo, J.; Sun, Y.; Moses, D.; Wudl, F.; Heeger, A. J. *Adv. Mater.* **2011**, *23*, 2272.
(12) Karadas, F.; Shatruk, M.; Perez, L. M.; Dunbar, K. R. *Chem.—Eur. J.* **2010**, *16*, 7164.
(13) Zhou, M.; Pfennig, B. W.; Steiger, J.; Van Engen, D.; Bocarsly, A. B. *Inorg. Chem.* **1990**, *29*, 2456−2460.
(14) Watson, D. F.; Tan, H. S.; Schreiber, E.; Mordas, C. J.; Bocarsly, A. B. *J. Phys. Chem. A* **2004**, *108*, 3261.
(15) Funck, K. E.; Prosvirin, A. V.; Mathoniere, C.; Clerac, R.; Dunbar, K. R. *Inorg. Chem.* **2011**, *50*, 2782.
(16) Lynch, M. S.; Van Kuiken, B. E.; Daifuku, S. L.; Khalil, M. *J. Phys. Chem. Lett.* **2011**, *2*, 2252.
(17) Lynch, M. S.; Cheng, M.; Van Kuiken, B. E.; Khalil, M. *J. Chem. Phys.* **2012**, *136*, 241101.
(18) Slenkamp, K. M.; Lynch, M. S.; Van Kuiken, B. E.; Brookes, J. F.; Bannan, C. C.; Daifuku, S. L.; Khalil, M. *J. Chem. Phys.* **2014**, *140*, 084505.
(19) Pfennig, B. W.; Bocarsly, A. B. *J. Phys. Chem.* **1992**, *96*, 226.
(20) Chang, C. C.; Pfennig, B.; Bocarsly, A. B. *Coord. Chem. Rev.* **2000**, *208*, 33.
(21) Watson, D. F.; Bocarsly, A. B. *Coord. Chem. Rev.* **2001**, *211*, 177.
(22) Becke, A. D. *J. Chem. Phys.* **1993**, *98*, 5648.
(23) Lee, C.; Yang, W.; Parr, R. G. *Phys. Rev. B* **1988**, *37*, 785.
(24) Mennucci, B.; Tomasi, J. *J. Chem. Phys.* **1997**, *106*, 5151.
(25) Lange, A. W.; Herbert, J. M. *J. Chem. Phys.* **2010**, *133*, 244111.
(26) Lange, A. W.; Herbert, J. M. *Chem. Phys. Lett.* **2011**, *509*, 77−78.
(27) Dolg, M.; Stoll, H.; Preuss, H. *J. Phys. Chem.* **1993**, *97*, 5852.
(28) de Berredo, R. C.; Jorge, F. E. *J. Mol. Struct.* **2010**, *961*, 107.
(29) Stein, T.; Kronik, L.; Baer, R. *J. Chem. Phys.* **2009**, *131*, 244119.
(30) Marcus, R. A. *Rev. Mod. Phys.* **1993**, *65*, 599.
(31) Krylov, A. I.; Gill, P. M. *WIREs Comput. Mol. Sci.,* **2013**, *3*, 317.
(32) Pfennig, B. W.; Lockard, J. V.; Cohen, J. L.; Watson, D. F.; Ho, D. M.; Bocarsly, A. B. *Inorg. Chem.* **1999**, *38*, 2941.
(33) Voityuk, A. A.; Rösch, N. *J. Chem. Phys.* **2002**, *117*, 5607.
(34) Cave, R. J.; Newton, M. D. *Chem. Phys. Lett.* **1996**, *249*, 15.
(35) Wu, Q.; Van Voorhis, T. *J. Chem. Theor. Comput.* **2006**, *2*, 765.
(36) Wu, Q.; Van Voorhis, T. *J. Phys. Chem. A* **2006**, *110*, 9212.